Semiconductor Physics, Quantum Electronics & Optoelectronics. 2003. V. 6, N 2. P. 227-232.

PACS: 72.80.Ey

Studies of CdHgTe as a material for *x*- and γ-ray detectors

L.A. Kosyachenko, V.V. Kulchynsky, O.L. Maslyanchuk, S.Yu. Paranchych, V.M. Sklyarchuk
Chernivtsi National University, 2 Kotsyubinsky str., 58012 Chernivtsi, Ukraine
e-mail: lakos@chv.ukrpack.net

Abstract. Optical, electric and photoelectric properties of $Cd_{1-x}Hg_xTe$ alloy with a low Hg content ($x = 0.05$) have been studied. The depth of impurity levels determining the conductivity of the material, their concentration and compensation degree, as well as the carrier lifetime and surface-recombination velocity have been found.

Keywords: CdHgTe alloy, radiation detectors, conductivity, carrier lifetime.

Paper received 25.05.03; accepted for publication 16.06.03.

1. Introduction

For several decades cadmium telluride (CdTe) has served as a basis for semiconductor *x*-ray and γ-detectors with quantum energy range extended as compared to silicon detectors (up to ~1 MeV) [1–3]. One of the key characteristics of the material utilized is electric conductivity that should be close to intrinsic. CdTe single crystals (mostly of *p*-type) prepared by current techniques are characterized by a considerable concentration of residual impurities and crystal lattice defects (up to 10^{15}–10^{16} cm^{-3}), therefore semi-insulating behaviour is usually achieved by donor compensation (for example, by Cl doping). In the mid-1990s it was found that $Cd_{1-x}Zn_xTe$ ($x \approx 0.1$) single crystals grown by a high-pressure Bridgman method are less defective as compared to CdTe [4,5]. Nevertheless, the problem of reproducibility both of CdTe and $Cd_{1-x}Zn_xTe$ conductivity remains relevant, and the search for materials for *x*- and γ-detectors goes on.

CdTe-HgTe alloy with HgTe content about 80% is well studied in connection with its use in the infrared radiation detectors for the wavelength range of 8–14 μm. However, the material with a low HgTe content, potentially suitable for the use in *x*-and γ-detectors, is practically unstudied. Attractive, among other things, is the narrowing of bandgap E_g (as compared to CdTe) resulting from Hg introduction to the crystal lattice (in contrast to the extension of E_g in $Cd_{1-x}Zn_xTe$ resulting from Zn introduction), as long as it leads to reduction of the average energy of atom ionization by a high-energy quantum. The reduction of resistivity caused by narrowing of the bandgap can be compensated by thermoelectric cooling used in CdTe and $Cd_{1-x}Zn_xTe$ detectors [6].

Below are the results of studying $Cd_{1-x}Hg_xTe$ single crystals with the bandgap 1.37 eV ($x = 0.05$). From optical, electric and photoelectric measurements, the parameters, which determine the material resistivity and the efficiency of carrier collection in x- and γ-detectors, have been found: the energy-level depth of impurities (crystal-lattice defects), the compensation degree, the carrier lifetime and the surface-recombination velocity.

2. Samples

$Cd_{1-x}Hg_xTe$ ($x = 0.05$) single crystals of *p*-type were grown by a vertical Bridgman method. In the growth process, the crystals were vanadium (V) doped (10^{18} cm^{-3}). The introduction of V produces deep levels near the middle of the bandgap, which together with the compensating action of other impurities and defects leads to the increase in the material resistivity [7]. As shown by our optical measurements, Hg content in various ingot parts proved to be somewhat different. The resistivity of samples was also different. The results shown below were obtained on the wafers cut from the middle-ingot part.

The bandgap of the material E_g was found from the optical transmission spectra for the plates with mirror surfaces. From the measured transmission T the absorption coefficient α was found by the formula taking into account multiple reflections in the sample:

$$\alpha = \frac{1}{d}\ln\left\{\frac{(1-R)^2}{2T} + \left[\frac{(1-R)^4}{4T^2} + R^2\right]^{1/2}\right\} \qquad (1)$$

where d is the plate thickness, and R is the reflectivity slightly varied within the edge of intrinsic absorption and assumed equal to 0.22 in the calculation [8].

As long as interband transitions in $Cd_{1-x}Hg_xTe$ are direct, for the determination of E_g the absorption curves $\alpha(h\nu)$ were plotted in coordinates α^2 versus the photon energy $h\nu$. As is seen from Fig. 1, a relatively slow variation of α in the transparency region of the crystal is going to its drastic increase at $h\nu > 1.35$ eV. In the region where $\alpha > 100$ cm^{-1}, a linear portion of the curve intersects the abscissa axis at the energy $E_g = 1.37$ eV. According to the empirical dependence of the $Cd_{1-x}Hg_xTe$ bandgap on the mercury content and temperature $E_g(x,T) = -0.302 + 1.93x + 5.35\times10^{-4}T(1-2x) - 0.81x^2 + 0.832x^3$ (which is well satisfied in the region of low x) [9] the value of E_g=1.37 eV is matched by $x = 0.05$.

Ohmic contacts for electric measurements were made by vacuum evaporation of Al at the substrate temperature of 200 °C. Prior to deposition, the crystal surface was treated by argon ions with the energy of 500 eV. It should be noted that high-quality ohmic contacts can be easier obtained with $Cd_{1-x}Hg_xTe$ than with CdTe. Good results are also achieved by vacuum gold evaporation and chemical copper deposition. High stability both of the bulk and the surface of samples has also engaged our attention. On keeping for more than a year the semi-insulating single crystals with the exposed surface have demonstrated no changes in their conductivity.

3. Conductivity of the crystals

Fig. 2 represents typical temperature dependences of resistivity ρ for two $Cd_{0.95}Hg_{0.05}Te$ single crystals with different values of ρ at room temperature.

Investigations made during recent decades have shown that mobilities of electrons μ_n and holes μ_p in intentionally undoped CdTe crystals at the temperatures above ~200 K are determined by deformation optical-phonon scattering and are given by expressions close to [10,11]:

$$\mu_n = 5.5\times10^6 T^{-3/2} \ \text{cm}^2/(\text{V·s}), \qquad (2)$$

$$\mu_p = 4\times10^5 T^{-3/2} \ \text{cm}^2/(\text{V·s}), \qquad (3)$$

whence follow quite real values $\mu_n = 1058$ cm^2/V·s and $\mu_p = 77$ cm^2/V·s at 300 K [5]. One can suppose that these expressions are also applicable to $Cd_{1-x}Hg_xTe$ with a *low* Hg content, i.e., the electron and hole mobilities are proportional to $T^{-3/2}$. On the other hand, the effective densities of states in the conduction and valence bands, $N_c = 2(m_n^* kT/2\pi\hbar)^{3/2}$ and $N_v = 2(m_p^* kT/2\pi\hbar)^{3/2}$ the expression for resistivity

$$\rho = \frac{1}{en\mu_n + ep\mu_p} \qquad (4)$$

are proportional to $T^{3/2}$ (m_n^* and m_p^* are the effective masses, n and p are the concentrations of electrons and holes, respectively). Thus, the temperature dependence of the resistivity is determined by exponential factors of the type $\exp(-\Delta E/kT)$, i.e., the slope of the $\rho(T)$ dependence plotted as $\log\rho$ versus $1000/T$ yields the *activation energy* of the conductivity ΔE that for crystals with resis-

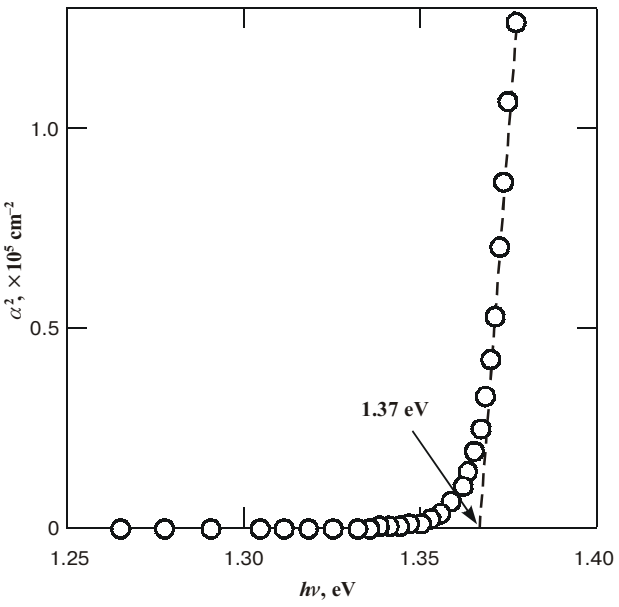

Fig. 1. Spectral dependence of absorption in the $Cd_{0.95}Hg_{0.05}Te$ single crystal at 300 K.

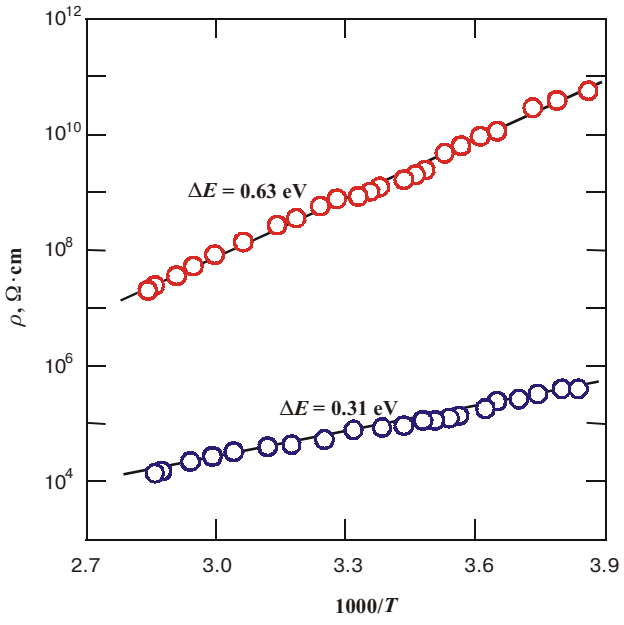

Fig. 2. Temperature dependences of resistivity ρ for the $Cd_{0.95}Hg_{0.05}Te$ crystal with $\rho = 9\times10^4$ and 1×10^9 Ω·cm at 300 K.

tivity 9×10^4 and 1×10^9 Ohm·cm is equal to 0.31 eV and 0.63 eV, respectively.

The conductivity of CdTe single crystals and alloys close in composition to CdTe (for example, $Cd_{1-x}Zn_xTe$) is determined by impurities and crystal lattice defects whose concentration can reach 10^{15}–10^{16} cm^{-3} [12,13]. Applying the same approach to the single crystals under study, one should take into account the compensation effects, as long as both the donor and acceptor levels were found in the bandgap. Consideration of statistics of electrons and holes in *p*-type semiconductor leads to two characteristic temperature dependences of the hole concentration [14,15]:

$$p \approx \frac{N_a - N_d}{N_d} N_v \exp\left(-\frac{E_a}{kT}\right) \tag{5}$$

$$p \approx \sqrt{N_a N_v}\, \exp\left(-\frac{E_a}{2kT}\right) \tag{6}$$

at high and low compensation degrees, respectively (N_a and N_d are the acceptor and donor concentrations).

Conspicuous is the fact that the slopes of the straight lines in Fig. 2 are almost 2-fold different. Hence, it can be supposed that the samples with high and low resistivity correspond to strong and weak compensation of the *same* acceptor, respectively. In conformity with Eqs. (5) and (6), in the first case the activation energy ΔE is equal to the acceptor *ionization energy* E_a, whereas in the second case $\Delta E = E_a/2$. This assumption is proved by an analysis of temperature variation in the Fermi level position for the samples under study.

Measuring the Fermi level energy $\Delta\mu$ from the valence-band top (Fig. 3), for the electron and hole concentrations in the conduction and valence bands one can write:

$$n = N_c \exp\left(-\frac{E_g - \Delta\mu}{kT}\right) \tag{7}$$

$$p = N_v \exp\left(-\frac{\Delta\mu}{kT}\right) \tag{8}$$

(Since the conductivity of sample with a high resistivity is close to intrinsic, one has to take into account both the electron and hole components in Eq. (1)). Solving Eq. (1) for $\Delta\mu$, with allowance made for Eqs. (2), (3), (5) and (6), yields

$$\Delta\mu = kT \ln\left(\frac{1-\sqrt{1-4e^2\rho^2\mu_n\mu_p n_i^2}}{2e\rho\mu_n n_i^2/N_v}\right) \tag{9}$$

where $n_i = (N_c N_v)^{1/2}\exp(-E_g/2kT)$ is the intrinsic carrier concentration.

The circles in Fig. 4 indicate the temperature dependences of the Fermi energy level $\Delta\mu(T)$ found from the measured curves $\rho(T)$ by the formula (9). As can be seen, for the two samples there is qualitative difference in the behaviour of the curves $\Delta\mu(T)$ that might be expected bearing in mind the difference in the compensation degrees in both cases. The conductivity of sample with a higher resistivity is close to intrinsic for $Cd_{0.95}Hg_{0.05}Te$ ($\rho = 2\times10^9$ Ohm·cm at 300 K), but the Fermi level is located slightly lower than the middle of the bandgap, i.e., the semiconductor has a weakly expressed *p*-type conductivity.

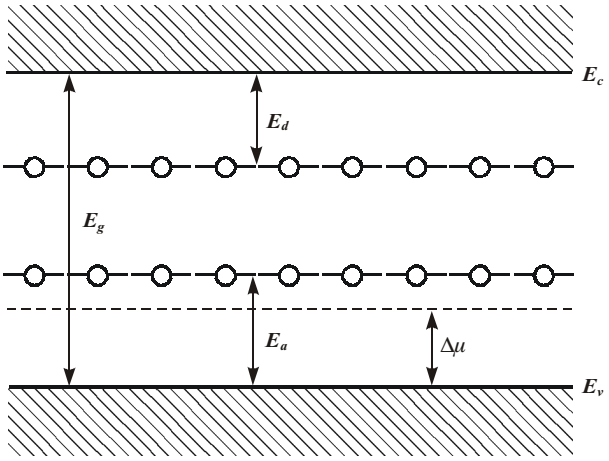

Fig. 3. Energy levels of impurities (defects) in the compensated semiconductor discussed in the work.

Let us consider a semiconductor with an acceptor level located by E_a above the top of the valence band and a donor level located by E_d below the bottom of the conduction band (E_a and E_d is the acceptor and donor *ionization energy*, respectively). As before, we shall denote the acceptor and donor concentrations by N_a and N_d. In the chosen calculation system, the concentrations of ionized acceptors N_a^- and donors N_d^+ can be expressed as

$$N_d^+ = \frac{N_d}{\exp\left(-\dfrac{E_g - E_d - \Delta\mu}{kT}\right)+1} \tag{10}$$

$$N_a^- = \frac{N_a}{\exp\left(\dfrac{E_a - \Delta\mu}{kT}\right)+1} \tag{11}$$

(degeneracy factors are omitted, which is equivalent to introducing only a small error into the value of impurity ionization energy). The Fermi energy level $\Delta\mu$ is found from the electroneutrality condition that for the model under consideration is of the form

$$n + N_a^- = p + N_d^+ \tag{12}$$

Based on the assumption made, we shall take the depth of the acceptor level $E_a = 0.63$ eV. The compensating effect of donor is independent of the value E_d, if its level is located several kT above the acceptor level. For certainty, we shall take $E_d = 0.1$ eV. We shall also take the acceptor concentration N_a equal to 10^{16} cm^{-3} (in conformity with Eq. (5), in the temperature range under study the results of calculations do not depend on the value N_a, but only on its relation to N_d).

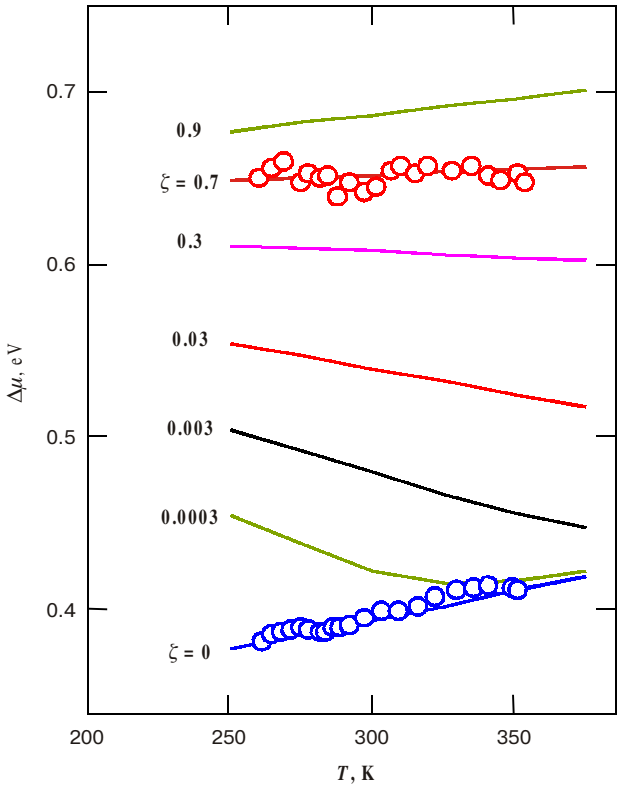

Fig. 4. Temperature dependences of the Fermi level energy (measured from the top of the valence band) calculated by Eq. (9) (solid lines) and obtained from the curves $\rho(T)$ presented in Fig.2 (circles).

Setting different values of E_g, E_a, E_d, N_a, one can now calculate the curves $\Delta\mu(T)$, using donor concentration N_d as a parameter. The results of such a calculation for different values of $\xi = N_d/N_a$ are represented in Fig. 4 by solid lines. As can be seen, the values of $\Delta\mu$ found from the experimental dependences $\rho(T)$ are in a good agreement with the calculated curves for $\xi = 0.7$ and $\xi \approx 0$ for the samples with a high and low resistivity, respectively. Thus, the assumption as to the mechanism of compensated impurity conductivity is justified and, what is more, correlation between the experimental and calculation results makes it possible to determine the degree of compensation for the samples under study. The measured curve $\rho(T)$ for weakly compensated sample with Eq. (6) also allows to determine the acceptor concentration N_a. This concentration has turned out to be equal to 7×10^{15} cm^{-3} that is in good agreement with the data reported elsewhere [12,13].

Naturally, in addition to the level considered above, the existence of other levels in the semiconductor bandgap must not be ruled out either. However, the Fermi level position, hence the electric conductivity, in compensated semiconductor, are completely determined by *partially* compensated deep level. Less deep levels ($E_a < 0.35$ eV, see Fig. 3) are *completely* compensated and do not affect the process of compensation of deeper levels. Similarly, one may not consider the levels located several kT above the partially compensated level, since their occupation with electrons need not be taken into account.

In the above calculations, the temperature variation of the semiconductor bandgap was ignored. The inclusion of this variation, would also necessitate taking into account the temperature dependence of the level depth in the bandgap. On the other hand, it would only introduce some corrections into the resulting semiconductor parameters because of the relatively narrow temperature range used (270–350 K).

4. Lifetime and surface recombination velocity

Along with electric conductivity, the carrier lifetime is a most critical parameter of a semiconductor utilized in *x*- and γ-detector. The small lifetime value in CdTe and $Cd_{1-x}Zn_xTe$ restricts the efficiency of collection of carriers produced by absorbed quantum, owing to which a fairly high voltage has to be applied to the detector (several hundreds of volts for the crystal thickness of several millimeters), leading to undesirable increase in the "dark" current.

The carrier lifetime can be found by measuring photoconductivity in the region of fundamental semiconductor absorption, i.e., phenomenon based on the intrinsic photoeffect like detection of *x*- and γ-quantums. (Compton scattering and generation of electron-positron pairs by the absorbed high-energy quantum is of minor importance). It is also important that the photoconductivity can be investigated using the crystal cut for *x*- and γ-detector and supplied with the same ohmic contacts. Besides, photoconductivity, like collection of carriers when detecting *x*- and γ-quantums, is adversely affected by the surface recombination.

Let us consider photoconductivity of plate of thickness d irradiated by photon flux Φ_0 (the number of photons incident on the unit area per unit of time), as is shown in Fig. 5.

The photon flux decreases along coordinate x as $\Phi(x) = \Phi_0\exp(-\alpha x)$, and the velocity of the electron-hole pairs generation $g(x)$ as $g(x) = -d\Phi/dx = \Phi_0\alpha\cdot\exp(-\alpha x)$. In section x, the electric current density is determined by carrier drift and diffusion:

$$j_n = eF\mu_n n + eD_n\frac{dn}{dx} \tag{13}$$

where F is the electric-field strength, and D_n is the electron diffusion coefficient.

Under steady-state conditions the surface recombination on the front and back surfaces (sections $x = 0$ and $x = d$) is compensated by inflow of electrons and holes. Therefore

$$S_n\Delta n(0) = \frac{1}{e}j_n(0) = D_n\frac{d\Delta n(0)}{dx} \tag{14}$$

$$S_n\Delta n(d) = \frac{1}{e}j_n(d) = D_n\frac{d\Delta n(d)}{dx} \tag{15}$$

where S_n is the surface recombination velocity, and Δn is the excess electron concentration equal to the excess hole concentration for interband transitions.

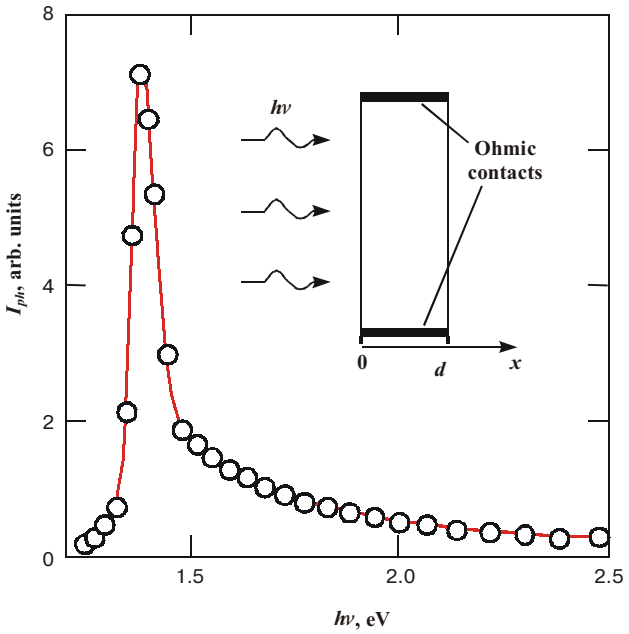

Fig. 5. Photoresponse spectrum of $Cd_{0.95}Hg_{0.05}Te$ crystal at 300 K. The insert shows the schematic diagram of a semiconductor slab with two ohmic contacts.

From the continuity equation for electrons

$$g - \frac{1}{e}\frac{dj_n}{dx} - \frac{\Delta n}{\tau_n} = D_n \frac{d^2\Delta n}{dx^2} - \frac{\Delta n}{\tau_n} + \Phi_0 \alpha \exp(-\alpha x) = 0 \tag{16}$$

with regard for (13), (14), (15) and (16) one can find the excess electron concentration $\Delta n = \Delta n(x, \alpha)$. The total number of excess electrons (related to unit area of irradiated surface) is found by integration of $\Delta n(x)$ from 0 to d. Solution of similar equations can be found elsewhere [16,17]:

$$\Delta n(\alpha) = \int_0^d \Delta n(x,\alpha) = \Phi_0 \tau_n \frac{1-\exp(-\alpha d)}{1+\frac{S_n\tau_n}{L_n}\coth\left(\frac{d}{2L_n}\right)} \times \left(1+\frac{S_nL_n}{D_n}\frac{\coth\left(\frac{d}{2L_n}\right)-\alpha L_n \coth\left(\frac{\alpha d}{2}\right)}{1-\alpha^2 L_n^2}\right) \tag{17}$$

where $L_n = (\tau_n D_n)^{1/2}$ is the diffusion length of electrons (i.e., minority carriers).

The resulting expression is inconvenient for comparison to experiment if the lifetime and surface recombination velocity of carriers are unknown. However, it can be simplified using the fact that $\coth(y) \approx 1$ at $y \geq 5$. The diffusion length of electrons in CdTe and $Cd_{1-x}Zn_xTe$ cannot exceed 100 μm ($\tau_n = 10^{-6}$ s, $D_n = 25$ cm^2/s at 300 K), the detector thickness is generally 2–5 mm, therefore $\coth(d/2L_n) \approx 1$ and $\coth(\alpha d/2) \approx 1$ for $\alpha \geq 100$ cm^{-1}. Thus, in a wide variation range of $\alpha \geq 100$ cm^{-1} a simpler expression for $\Delta n(\alpha)$ is valid:

$$\Delta n(\alpha) = \Phi_0 \tau_n \frac{1-\exp(-\alpha d)}{1+\frac{S_n\tau_n}{L_n}}\left(1+\frac{S_nL_n}{D_n}\frac{1}{1+\alpha L_n}\right) \tag{18}$$

Letting α approach ∞, we obtain the value of Δn in the saturation region

$$\Delta n(\infty) = \Phi_0 \tau_n \frac{1}{1+\frac{S_n\tau_n}{L_n}} \tag{19}$$

and dividing $\Delta n(\infty)$ by $\Delta n(\alpha)$–$\Delta n(\infty)$, we obtain the value that is *linearly* dependent on α:

$$\frac{\Delta n(\infty)}{\Delta n(\alpha)-\Delta n(\infty)} = \frac{D_n}{S_nL_n}(1+\alpha L_n) \tag{20}$$

Thus, having the measured photoconductivity spectrum over a wide spectral range and using the slope and cutoff on the plot of $\Delta n(\infty)/[\Delta n(\alpha)–\Delta n(\infty)]$ versus α, one can determine the diffusion length of minority carriers (hence, their lifetime) and the surface recombination velocity. Note that to find these important parameters it will suffice to measure the photoconductivity in *relative* units (i.e., to use the spectral dependence of photocurrent $I_{ph}(h\nu)$).

Fig.5 shows the photoconductivity spectrum of $Cd_{0.95}Hg_{0.05}Te$ single crystal measured with allowance made for the photon number distribution at the exit slit of the spectral system. The spectral curve has a sharp maximum in the region of the intrinsic absorption edge (1.37–1.38 eV). With the increase in photon energy, a fairly rapid reduction in photosensitivity (evidence of surface recombination) with a tendency to saturation is observed, making it possible to determine the value of $\Delta n(\infty)$ appearing in Eq. (20).

The absorption curve $\alpha(h\nu)$ for the plates 100–200 μm thick can be obtained only for $\alpha < 200$–300 cm^{-1}. Expansion to the region of $\alpha = 10^5$–10^6 cm^{-1} using the transmission curves involves serious difficulties, as long as it requires the superthin plates, moreover, with their optical properties differing from those of bulk samples [18]. One can use, however, the fact that for alloys close in composition to CdTe, the absorption curves $\alpha(h\nu)$, found from the spectral dependences of the refraction $n(h\nu)$ and absorption indexes $\kappa(h\nu)$ as $\alpha = 2\omega\kappa/c$ (c is the light velocity in vacuum), *practically coincide* in the region of photon energy exceeding E_g by ~0.2 eV [8]. As compared to CdTe, the alloy absorption edge is shifted along the axis of photon energy by the appropriate value, but its behaviour $\alpha(h\nu)$ is also well reproducible. This allows to obtain the absorption curve $Cd_{0.95}Hg_{0.05}Te$ by "attaching" the measured absorption edge to the dependence $\alpha(h\nu)$ for CdTe taken from Ref. [8]. The results of this manipulation are shown in Fig. 6.

Fig. 6 also shows correlation of the measured photoconductivity spectrum for $Cd_{0.95}Hg_{0.05}Te$ single crystal

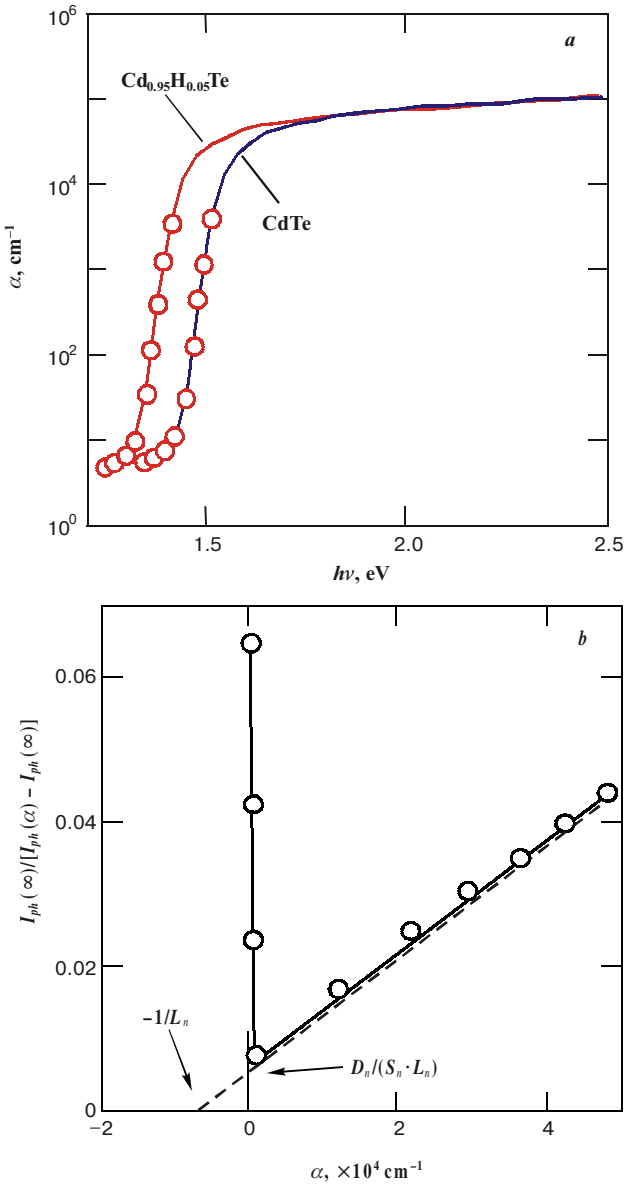

Fig. 6. *a* – The absorption curves for the $Cd_{0.95}Hg_{0.05}Te$ and CdTe crystals at 300 K. The circles show the results of measurements, the solid lines in the region $\alpha > 10^4$ cm^{-1} are taken from Ref. [8]. *b* – Correlation of the dependence $\Delta n(\alpha)$ with Eq. (20).

with Eq. (20). The excess electron concentration, as already mentioned, is replaced by photocurrent $I_{ph}(h\nu)$, and $I_{ph}(\infty)$ is used to denote its value in the region of large α (in the high-energy spectral region). As expected, on the resulting dependence, a section approximated by a straight line is observed. (At low α there is a sharp upward deviation where condition $\coth(\alpha d/2) \approx 1$ is not met.) The cutoffs of the straight line on the axes yield the surface-recombination velocity $S_n = (3–3.5)\times10^7$ cm/s, the electron diffusion length $L_n = 1.3–1.7$ μm, and the electron lifetime $\tau_n = (0.7–1.2)\times10^{-9}$ s ($D_n = 25$ cm^2/s at 300 K). Such a small value of τ_n is attributable to the presence of deep levels in the bandgap due to heavy V doping, which is also proved by the results of studying the surface-barrier structures on a similar material [19].

5. Conclusions

V-doped $Cd_{0.95}Hg_{0.05}Te$ single crystals with the bandgap 1.37 eV and the resistivity in the range from 10^4 to 10^9Ohm·cm at 300 K have been prepared. The conductivity mechanism of the crystals under study is of compensated impurity nature, and the difference in the conductivity of various ingot parts is caused by different compensation degrees. For conducting samples the compensation degree (N_d/N_a) is low, whereas for semi-insulating samples it reaches ~0.7. Measurement of the photoconductivity spectrum makes it possible to determine precisely the surface recombination velocity, diffusion length and minority carrier lifetime. The resulting electron lifetime in semi-insulating $Cd_{0.95}Hg_{0.05}Te$ is ~10^{-9} s.

References

1. Eiji Sakai. Present status of room temperature semiconductor detectors // *Nucl. Instr. and Meth.* **196**, pp. 121-130 (1982).
2. G. Entine, P. Waer, T. Tiernan, M.R. Squillante. Survey of CdTe nuclear detector applications // *Nucl. Instr. and Meth.* **A283**, pp. 282-290 (1989).
3. Y. Eisen. Current state-of-the-art applications utilizing CdTe detectors // *Nucl. Instr. and Meth.* **A322**, pp. 596-603 (1992).
4. J.F. Butler, C.L. Lingren, F.P. Doty. $Cd_{1-x}Zn_xTe$ gamma ray detectors // *IEEE Trans. Nucl. Sc.* **39**(4), pp. 605-609 (1992).
5. Y. Eisen, A Shor. CdTe and CdZnTe materials for room-temperature X-ray and gamma ray detectors// *J. Crystal Growth*. **184/185**, pp. 1302-1312 (1998).
6. R.H. Redus, A.C. Huber, J.A. Pantazis. Improved thermoelectrically cooled X/g-ray detectors and electronics // *Nucl. Instr. and Meth.* **A458**, pp. 214-219 (2001).
7. M. Fiederle, D. Ebling, C. Eiche, P. Hug, W. Joerger, M. Laasch, R. Schwarz, M. Salk, K.W. Benz. *J. Crystal Growth*. **146**, pp. 142-147 (1995).
8. T. Toshifumi, S. Adachi, H. Nakanishi, K. Ohtsuka. Optical constants of $Zn_{1-x}Cd_xTe$ Ternary alloys : Experiment and modeling // *Jpn. Appl. Phys.* **32**, pp. 3496-3501 (1993).
9. G.L. Hansen, J.L. Schmit, T.N. Casselman. Energy gap versus alloy composition and temperature in $Hg_{1-x}Cd_xTe$ // *J.Appl. Phys*. **53**, 7099-7101 (1982).
10. S.S. Devlin. Transport properties. In: Physics and Chemistry of II-VI Compounds. Eds. M. Aven, and J.S. Prener. North-Holland Publishing Gompany, New York, 1967. p.418.
11. I. Turkevych, R. Grill, J. Franc, E. Belas, P. Hoschl and P. Moravec. High-temperature electron and hole mobility in CdTe // *Semicond. Sc. Techn*. **17**, 1064 (2002).
12. D.M. Hofmann, W. Stadler, P. Chrismann, B.K. Meyer. Defects in CdTe and $Cd_{1-x}Zn_xTe$ // *Nucl. Instr. and Meth.* A**380**, 117-120 (1996).
13. A. Castaldini, A. Cavallini, B. Fraboni. Deep energy levels in CdTe and CdZnTe // *J. Appl. Phys*. **83**, 2121-2126 (1998).
14. J.S. Blakemore. *Semiconductor physics*. Pergamon Press, Oxford. pp. 139-140 (1962).
15. K. Seeger. *Semiconductor physics*. Springer-Verlag, Wien-New York. p. 67 (1973).
16. S.M. Sze. *Physics of semiconductor devices*. Wiley, New York. pp. 800-803 (1973).
17. A.I. Vlasenko, Z.K. Vlasenko, A.V. Ljubchenko. Photoconductivity spectral characteristics of semiconductors with an axponential edge of the fundamental absorption // *Semiconductors*. **33**, 1295-1299 (1999).
18. L.A. Kosyachenko, I.M. Rarenko, Z.I. Zakharuk, V.M. Sklyarchuk, E.F. Sklyarchuk, I.V. Solonchuk, I.S. Kabanova, E.L. Maslyanchuk. Electrical properties of CdZnTe surface-barrier diodes // *Semiconductors*. **37**, 227-232 (2003).
19. L.A. Kosyachenko, S.Yu. Paranchych, Yu.V. Tanasyuk, V.M. Sklyarchuk, Ye.F. Sklyarchuk, Ye.L. Maslyanchuk, V.V. Motushchuk. Generation-recombination centers in CdTe:V // *Semiconductors*. 37, pp. 452-455 (2003).